Electronic Supplementary Material (ESI) for Nanoscale Advances.
This journal is © The Royal Society of Chemistry 2023

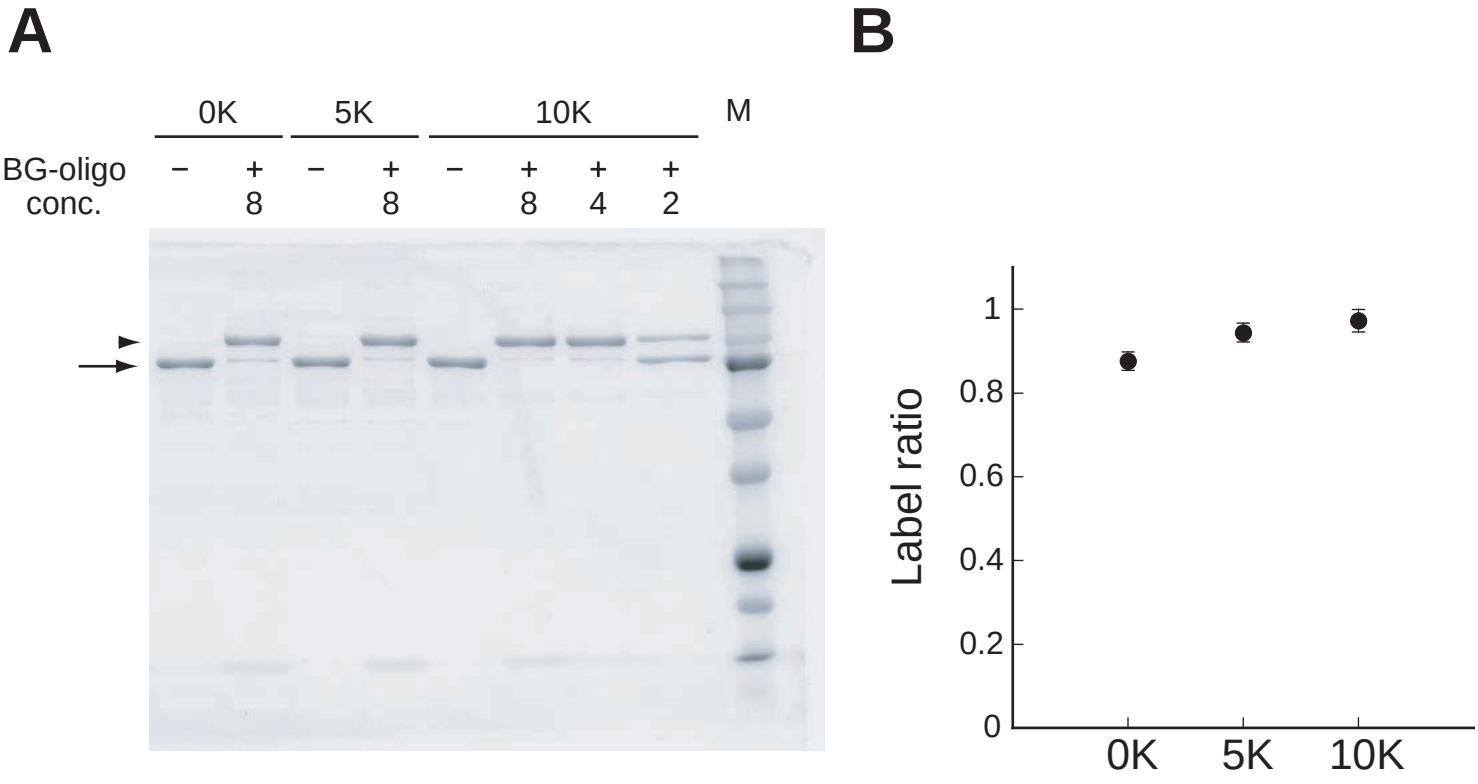

Supplementary Fig. 1. Lys-tag has minimal effect on the ligand binding ability of $SNAP_f$ protein. (A) SDS-PAGE mobility shift assay of kinesin-$SNAP_f$-Lys-tag bound to excess $SNAP_f$ substrate (oligo DNA with BG-handle, BG-DNA). Dimeric kinesin-$SNAP_f$-Lys-tag (1 mM) was incubated with BG-oligo DNA (2-8 mM) for 1.5 hours at 25°C. Arrow and arrowhead indicate free and BG-DNA-bound kinesin-$SNAP_f$, respectively. (B) Fractions of active $SNAP_f$ are more than 0.87, showing that Lys-tag has minimal effect on the ligand binding ability of $SNAP_f$ protein. Error bars indicate standard deviation of three independent experiments.

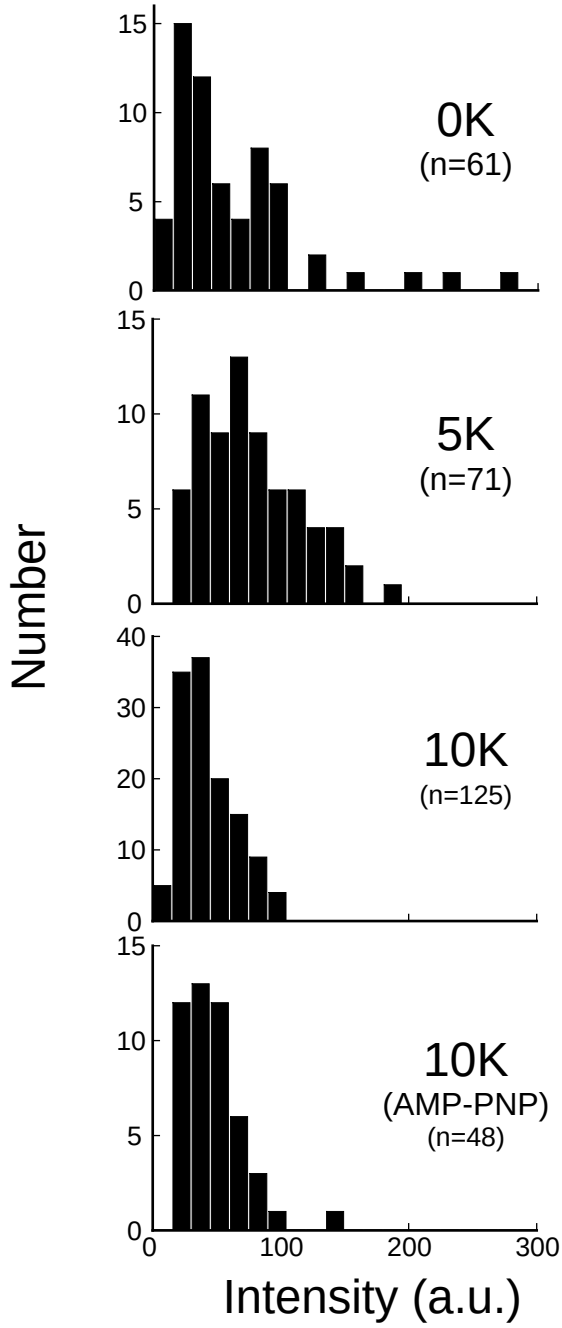

Supplementary Fig. 2. Single-molecule imaging of Lys-tagged kinesin.
Fluorescence intensity of kinesin-SNAP$_f$-Lys-tag labeled with Alexa Fluor 647 (A647-kinesin). A647-kinesins that moved along an axoneme at 1 mM ATP were analyzed. Median values (54, 74, and 42 for 0K, 5K, and 10K, respectively) are 1-2 times that of single A647 intensity (median value 42) estimated from photobleaching of A647-kinesin-10K immobilized on the axoneme at 2 mM AMP-PNP, indicating a single kinesin molecule.

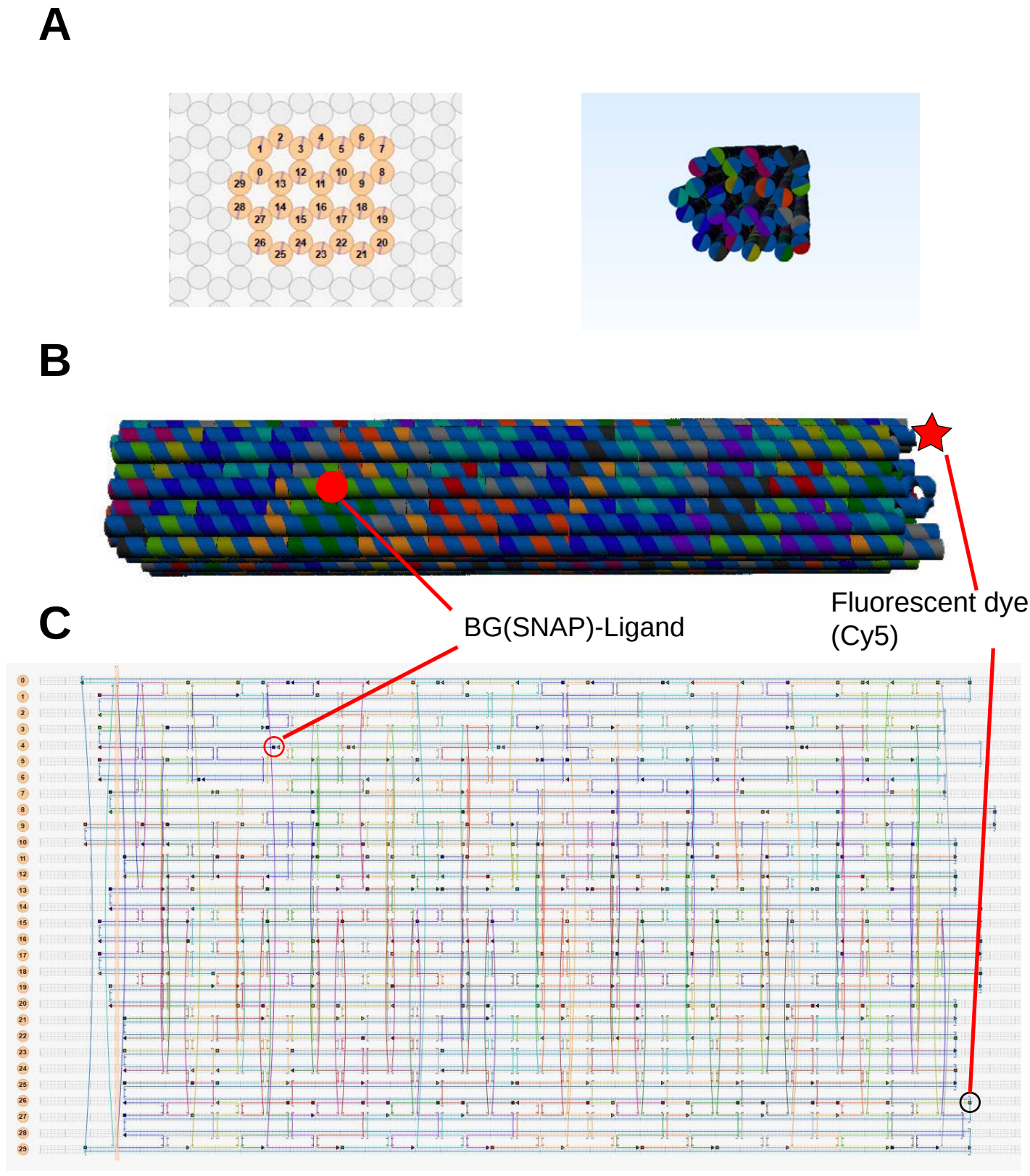

Supplementary Fig. 3. Structure and layout of the DNA rod (1-handle).
(A) Cross section image of caDNAno (left) and Maya (right). (B) Bottom view shows the position of the SNAP-ligand (red circle). (C) Secondary structure of the rod rendered using caDNAno.

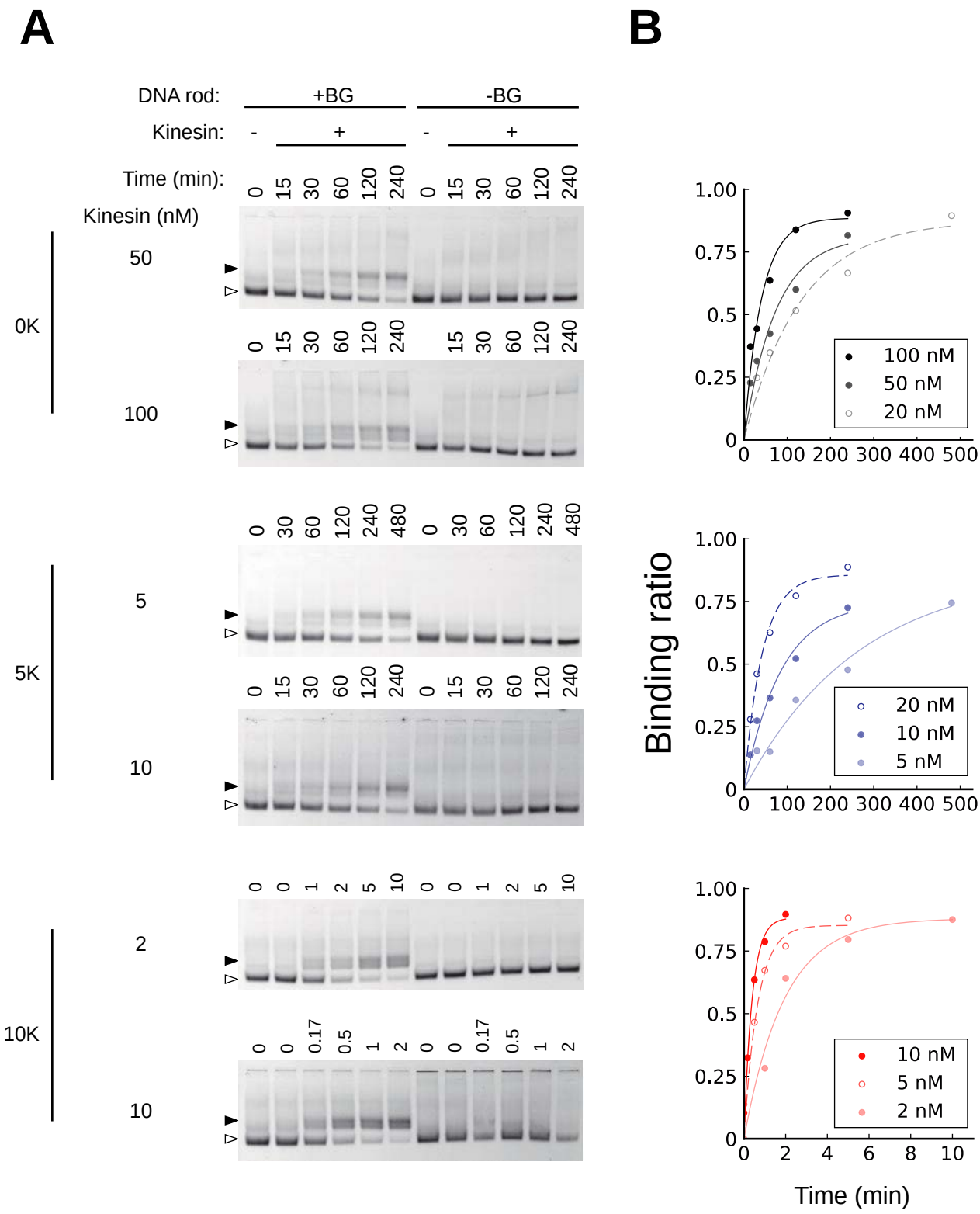

Supplementary Fig. 4. Lys-tag accelerates the speed of kinesin assembly on the DNA rod. (A) Results of 0.7% agarose gel electrophoresis as in Fig. 2B, except for difference in kinesin concentration. Open- and closed-arrowheads indicate free- and kinesin-bound DNA rods, respectively. (B) Quantifications of agarose gel data in (A) are shown with closed plots and solid lines. For reference, data in Fig. 2C are shown with open plots and dashed lines.

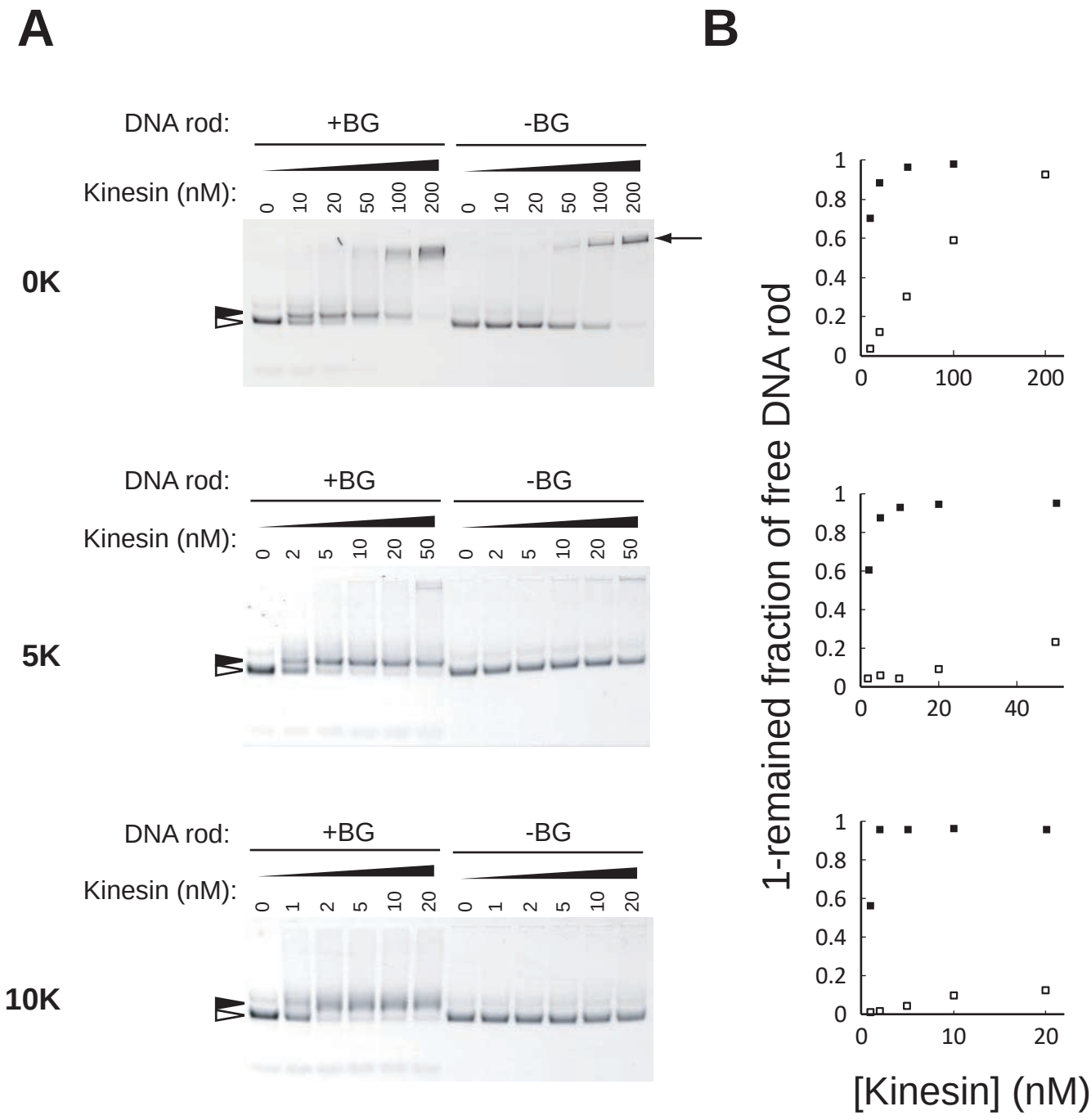

Supplementary Fig. 5. Lys-tag allows DNA rod-kinesin assembly without DNA rod aggregation. (A) Results of agarose gel electrophoresis show that high kinesin concentration accelerates DNA rod-kinesin assembly, but also accelerates DNA rod aggregation. DNA rod (2 nM) with or without the BG-handle were mixed with the indicated concentration of kinesins in 23 mM PIPES (pH 7.0), 0.8 mg/mL casein, 230 mM NaCl, 12 mM $MgCl_2$, 1 mM EGTA, 50 mM ATP and 1 mM DTT, and incubated for 8 hours (0K and 5K) or 3 hours (10K) at 25°C. Open- and filled-arrowheads indicate free- and kinesin-bound DNA rods. Arrow indicates aggregated DNA rod. (B) Quantification of (A). Fraction remaining of free DNA rod (open arrowhead in (A)) was measured and subtracted from 1. We noted that a reduction in DNA rods without a BG-handle is caused by DNA rod aggregation, whereas that of DNA rods with a BG-handle is caused both by aggregation and kinesin binding. 0K kinesin (without Lys-tag) requires high concentrations of kinesin for assembly, which leads to DNA rod aggregation (arrow on the right side of images), whereas 5K- and 10K-kinesin require low concentration for assembly, thereby avoiding the DNA rod aggregation.

A

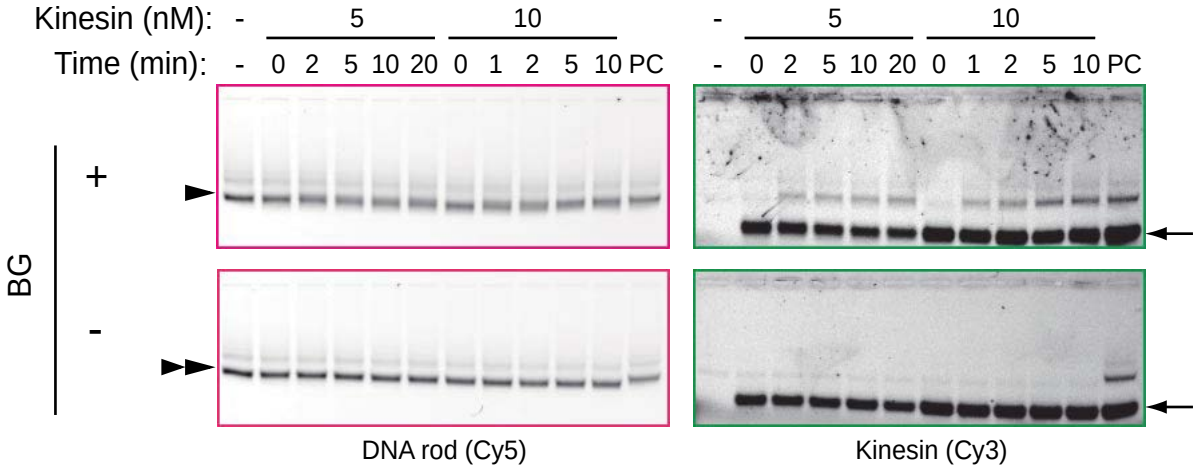

B

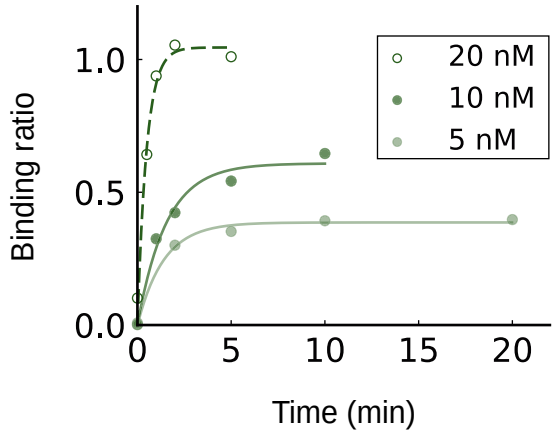

Supplementary Fig. 6. Lys-tag accelerated the speed of Cy3-kinesin assembly on the DNA rod (w/ SDS gel).
(A) Results of 0.7% agarose gel electrophoresis supplemented with 0.1% SDS as in Fig. 2C, except that 5 or 10 nM Cy3-kinesin-SNAP$_f$-10K was mixed with DNA rods with (top, arrowhead) or without (bottom, double arrowhead) a BG-handle. PC, DNA rod with a BG-handle were incubated for 20 minutes with kinesin-SNAP$_f$-10K (20 nM). Note that fluorescence signals of free kinesin (arrow) are saturated. (B) Quantifications of agarose gel data in (A) are shown in closed plots and solid lines. The data in Fig. 2D (20 nM) are shown in open plots and dashed lines. Fluorescence intensity of Cy3-kinesin was measured, and fluorescence intensity of positive control (PC) was set at 0.9.

A

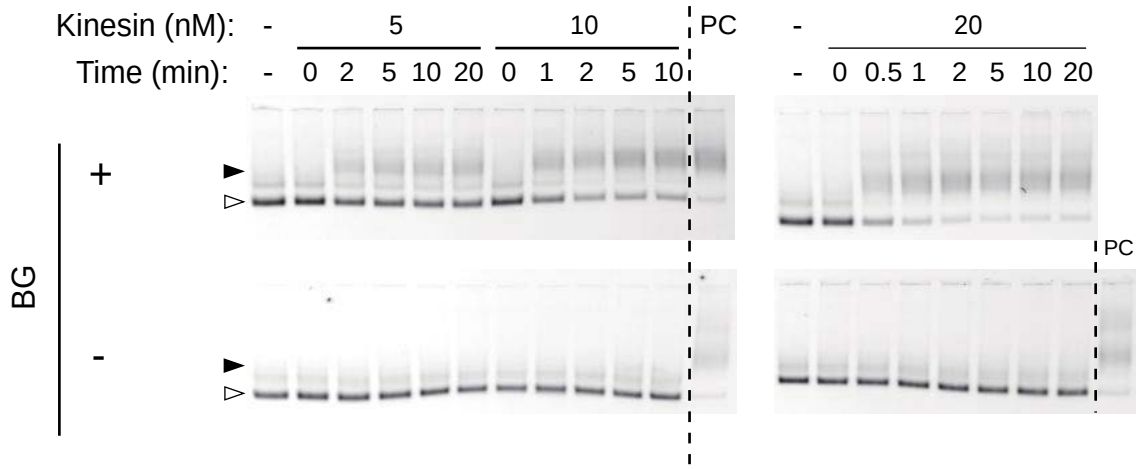

B

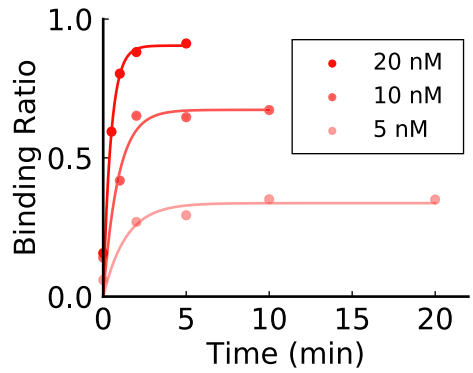

Supplementary Fig. 7. Lys-tag accelerated the speed of Cy3-kinesin assembly on the DNA rod (w/o SDS in the gel).
(A) Results of 0.7% agarose gel electrophoresis as in Fig. 2B, except that Cy3-kinesin-SNAP$_f$-10K was mixed with Cy5-DNA rod (5 nM) with or without a BG-handle. Open arrowheads and filled-arrowheads indicate free- and kinesin-bound Cy5-DNA rods, respectively. PC, DNA rod with a BG-handle were incubated for 20 minutes with kinesin-SNAP$_f$-10K (20 nM). (B) Quantifications of agarose gel data in (A) are shown in closed plots and solid lines. Fluorescence intensity of the Cy5-DNA rod was measured, and remaining fluorescence intensity of free-DNA rods was used for quantification.

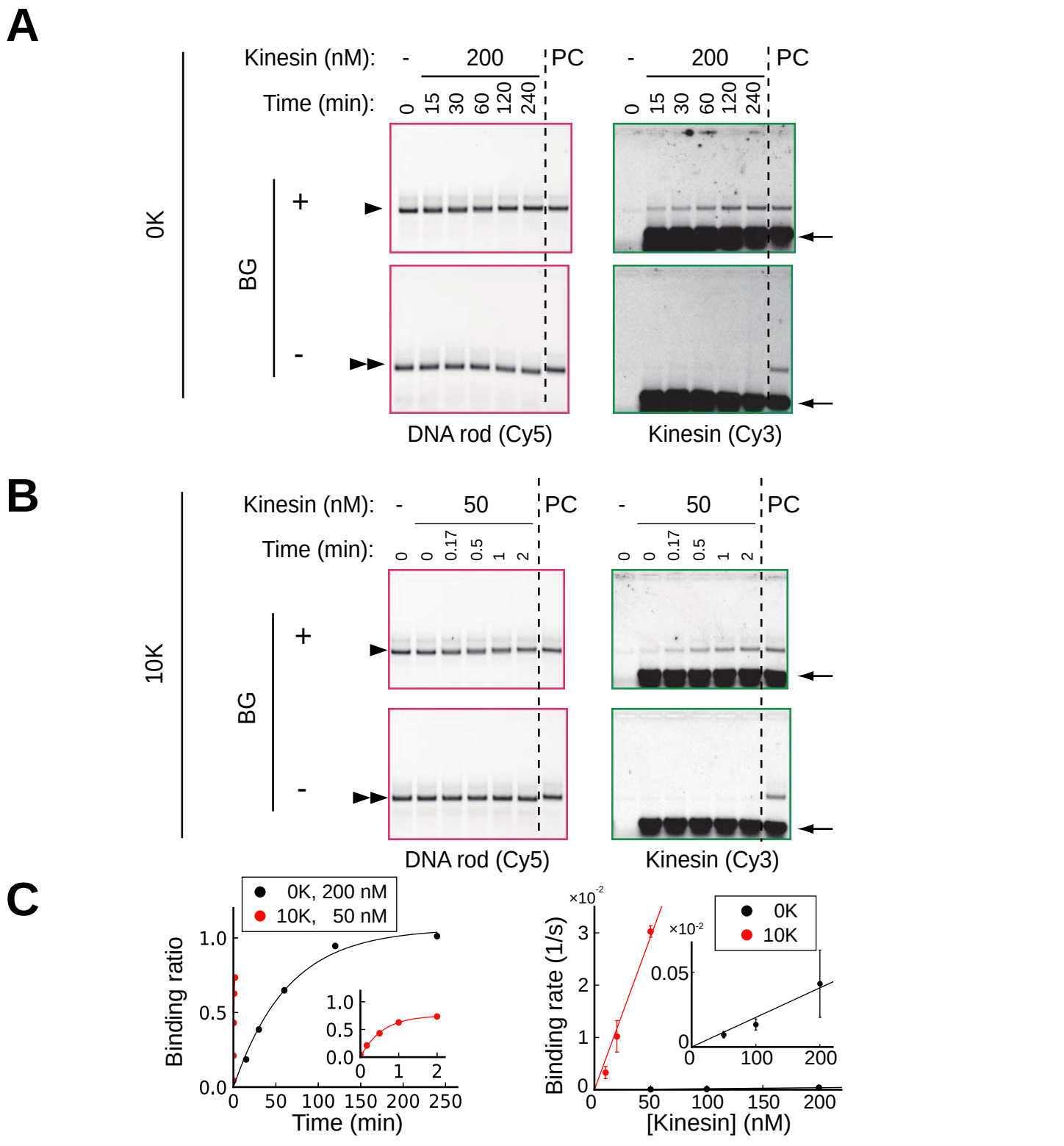

Supplementary Fig. 8. Lys-tag accelerates the speed of monomeric kinesin assembly on the DNA rod.

(A and B) Results of 0.7% agarose gel electrophoresis supplemented with 0.1% SDS as in Fig. 2D, except that monomeric kinesin-SNAP$_f$-0K (A) or -10K (B) labeled with Cy3 was mixed with DNA rods with (top, arrowhead) or without (bottom, double arrowhead) a BG-handle. PC, DNA rods with a BG-handle were incubated for 8 hours with 200 nM 0K (A) or for 20 minutes with 50 nM 10K (B). Note that fluorescence signals of free kinesin (arrow) are saturated. (C) Left, quantification of agarose gel data in (A and B). Right, results of three independent experiments show that Lys-tag accelerates assembly speed (K_{on} = 2 x 10^3 and 6 x 10^5 /M/s for 0K and 10K, respectively). Error bars indicate standard deviation of three independent experiments.

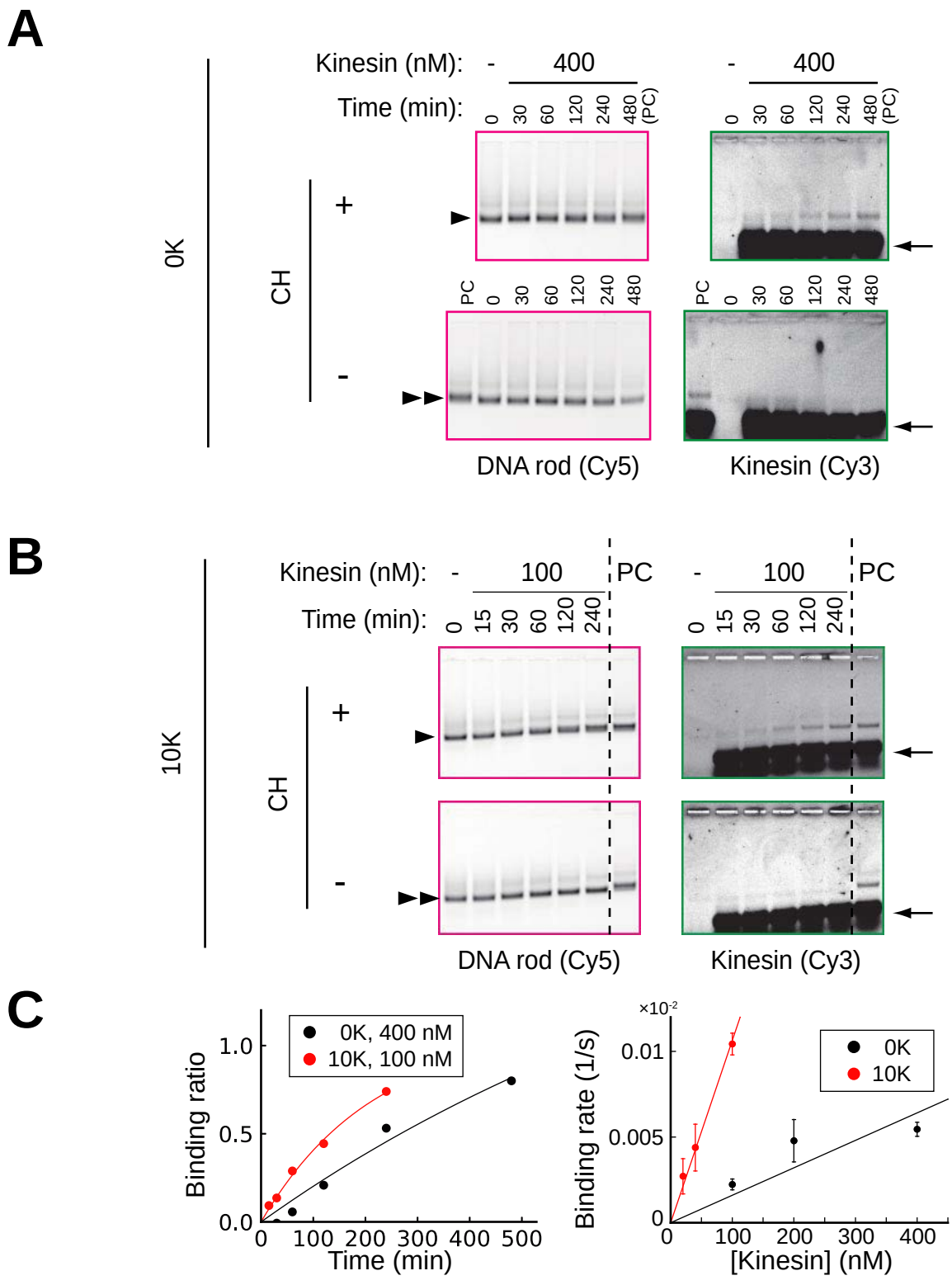

Supplementary Fig. 9. Lys-tag accelerates the speed of Halo-fused kinesin assembly on the DNA rod.

(A and B) Results of 0.7% agarose gel electrophoresis supplemented with 0.1% SDS as in Fig. 2D, except that kinesin-Halo-0K (A) or -10K (B) labeled with Cy3 was mixed with DNA rods with (top, arrowhead) or without (bottom, double arrowhead) a Halo-ligand handle (5-chlorohexane, CH). PC, DNA rods with a CH-handle were incubated for 8 hours with 400 nM 0K (A) or 100 nM 10K (B). Note that fluorescence signals of free kinesin (arrow) are saturated. (C) Left, quantifications of agarose gel data in (A) and (B). Right, results of three independent experiments show that Lys-tag accelerates assembly speed (K_{on} = 1 x 10^2 and 1 x 10^3 /M/s for 0K and 10K, respectively). Error bars indicate standard deviation of three independent experiments.

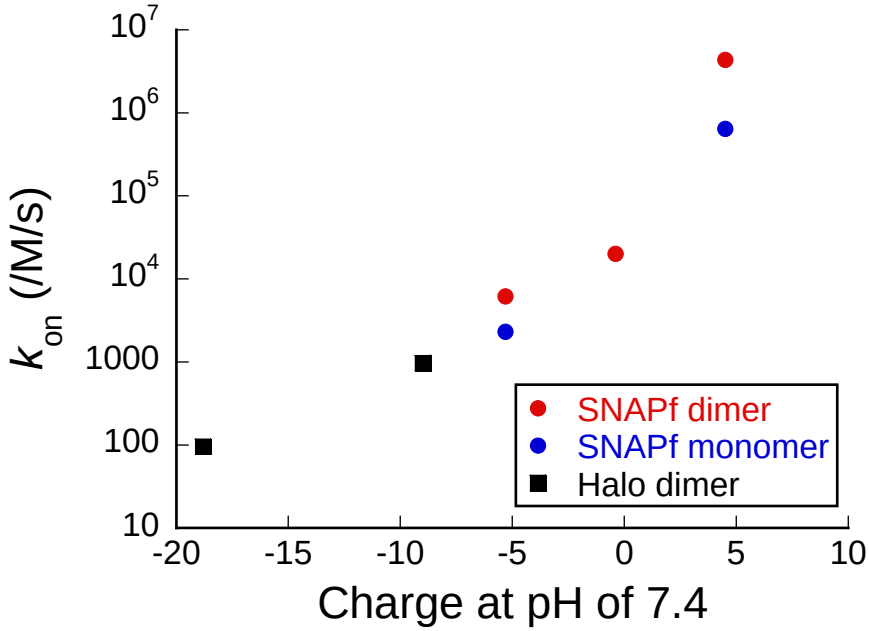

Supplementary Fig. 10. Relationship between the charge of tag-protein fragment and K_{on}. K_{on} values are plotted against the estimated charge of the tag-protein fragments, suggesting a relationship between K_{on} and fragment charge. Charge was estimated using the isoelectric point calculator (http://isoelectric.org/).

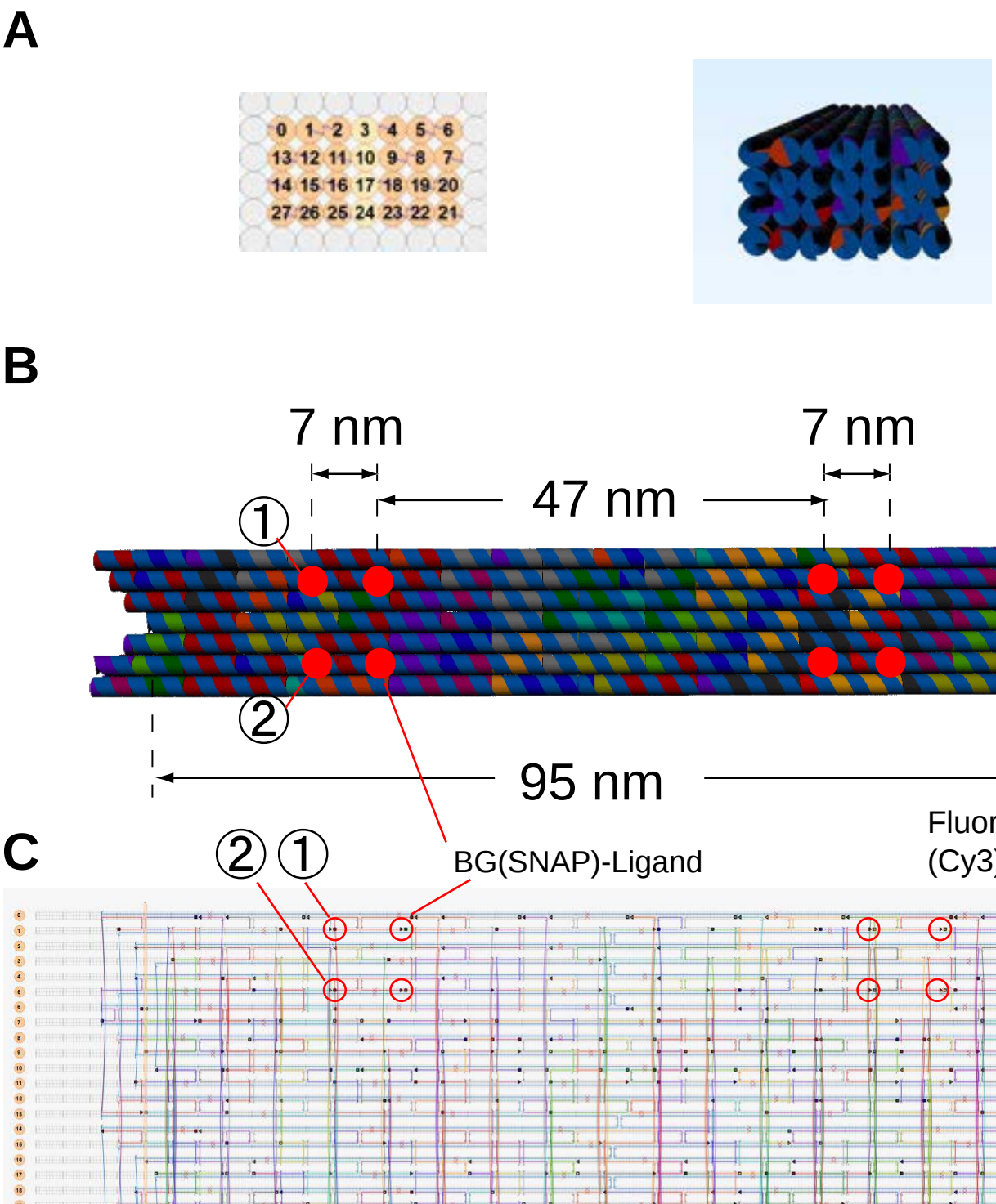

Supplementary Fig. 11. Structure and layout of the DNA rod (8-handle).
(A) Cross section image of caDNAno (left) and Maya (right). (B) Bottom view shows the position of the SNAP-ligand (red circle). (C) Secondary structure of the rod rendered using caDNAno.

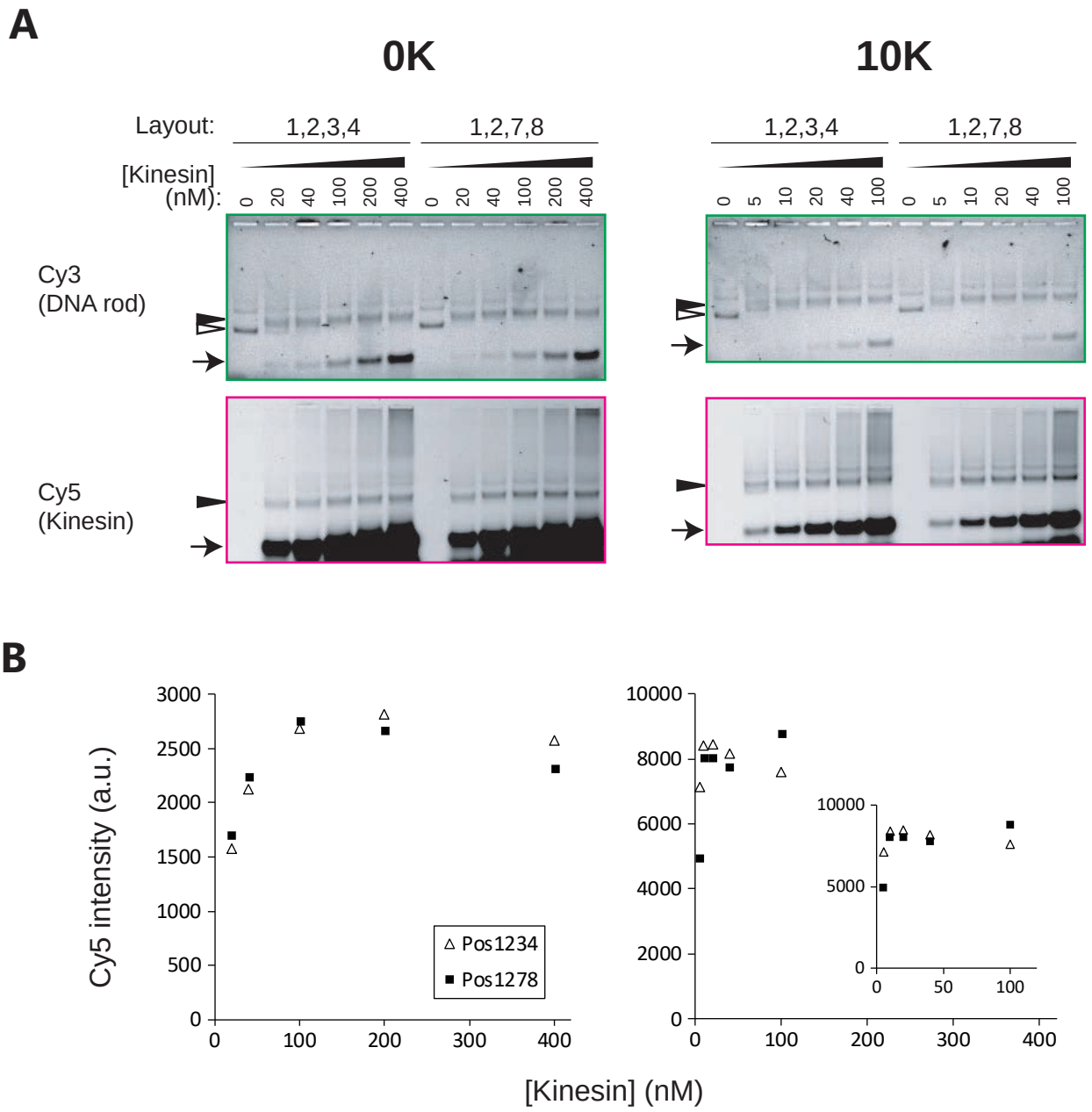

Supplementary Fig. 12. Lys-tag lowers the concentration of kinesin required.
(A) Assembly of Cy5-dimeric kinesin-SNAP$_f$-0K (left) or -10K (right) with different layouts of Cy3-DNA rods. DNA rods (2 nM) were mixed with the indicated concentration of kinesin in 23 mM PIPES (pH 7.0), 0.8 mg/mL casein, 230 mM NaCl, 12 mM $MgCl_2$, 1 mM EGTA, 50 mM ATP and 1 mM DTT, and incubated for 8 hours (0K) or 2 hours (10K) at 25°C. Open and filled arrowheads indicate free- and kinesin-bound DNA rods, respectively. Note that fluorescence signals of free kinesin (arrows) are saturated. (B) Quantification of the agarose gel data in (A). Maximal amounts of kinesin binding are similar for different layout DNA rods with 0K and 10K. By contrast, the required kinesin concentration of 10K (10 nM) is 10 times lower than that of 0K (100 nM). Cy5 intensities (kinesin) were corrected using Cy3 intensity (DNA rod). We noted that we did not calibrate the fluorescence intensity values of different gels, and thus did not compare the values of Cy5 intensity between 0K and 10K.

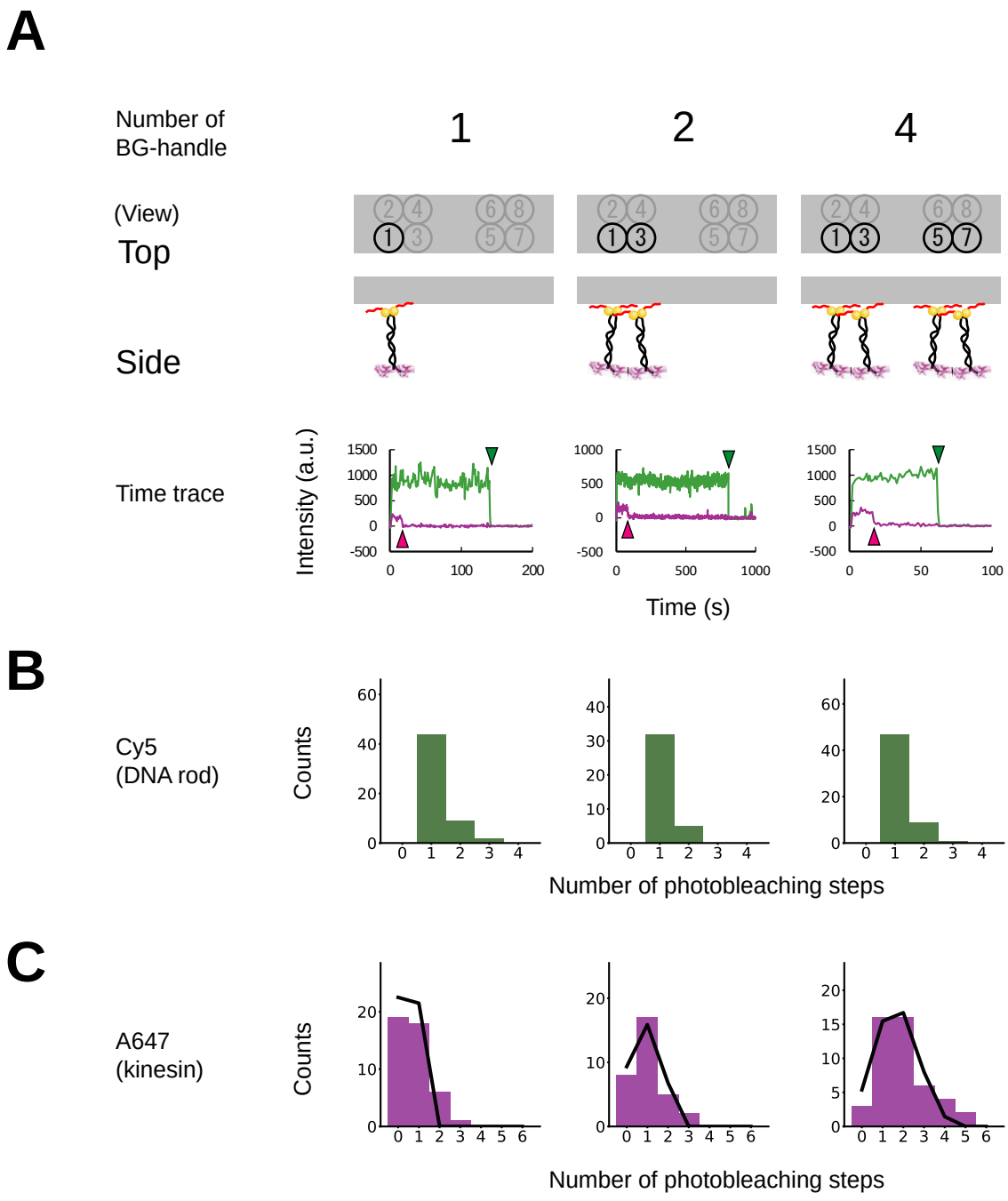

Supplementary Fig. 13. Fluorescence intensity analysis of a single kinesin-DNA rod complex. (A) Typical time traces of single step photobleaching of individual transport complexes. Cy3-labeled DNA rods with 1, 2, or 4 BG-handle(s) bound A647-labeled kinesin-SNAP$_f$-10K were attached to an axoneme at 2 mM AMP-PNP and 50 mM NaCl, and illuminated with two lasers (532 and 633 nm) a few seconds after starting image capture. Green- and magenta arrowheads indicate photobleaching of Cy3 (DNA rod) and A647 (kinesin), respectively. (B) Histograms of photobleaching step number of Cy3 (DNA rod). (C) Histograms of photobleaching step number of A647 (kinesin). Data of one step Cy3 photobleaching molecules were used. Occupancy fractions of A647-kinesin and number of A647-kinesin per site were estimated using a two-step process. First, A647 photobleaching step data were fitted with binomial distribution (solid lines) and estimated to be 0.49, 0.46, and 0.42 for 1, 2, and 4 BG-handle(s), respectively. Considering that DNA rod without kinesin does not bind the axonemes (data not shown), data for 1 BG-handle should reflect the DNA rod occupied with 1 kinesin (kinesin occupancy = 1). Therefore, occupancy fractions of kinesin of 2- and 4-BG handles could be converted from A647-dye occupancy data, and estimated to be 0.94 and 0.86, respectively.

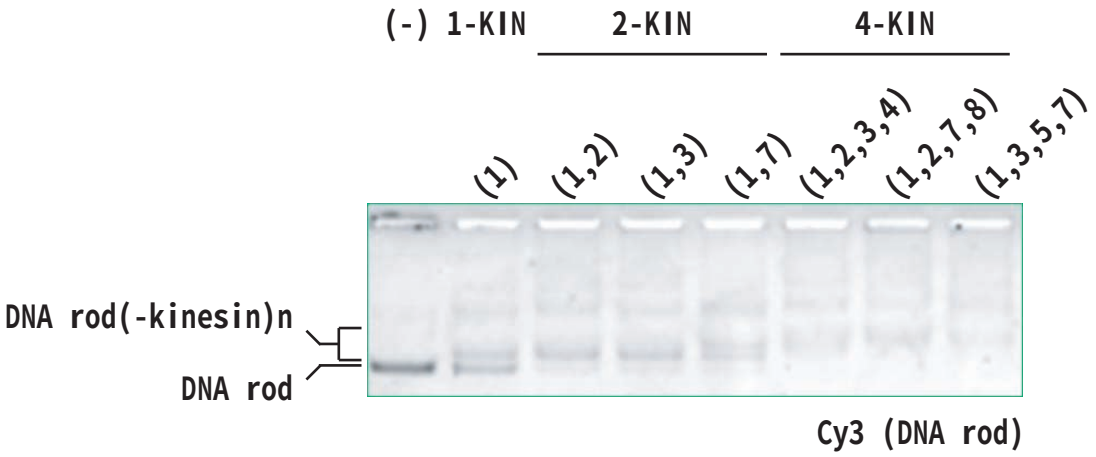

Supplementary Fig. 14. Mobility of DNA rods were shifted upon kinesin assembly.
DNA rods (2 nM) with 0, 1, 2, or 4 BG-handles incubated with A647-labeled dimeric kinesin-SNAP$_f$ (10 nM for 0 BG; at a BG/kinesin molar ratio of 1:5 for 1-4 BG). DNA rods with higher numbers of BGs had larger mobility shifts. Agarose gel supplemented with 0.001% SDS was used.

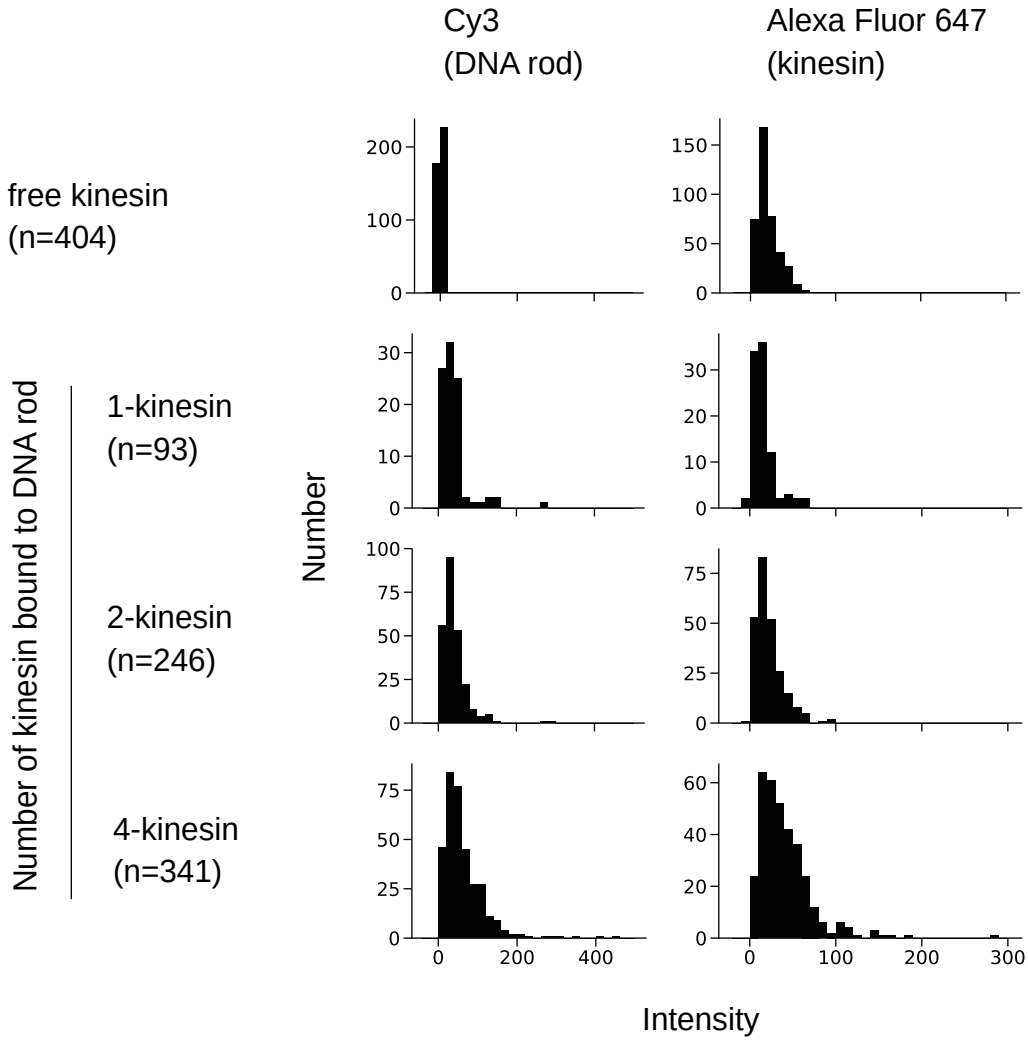

Supplementary Fig. 15. Fluorescence intensity distributions of kinesin-DNA rod in Fig. 3. Florescence intensities of transport complexes moving along an axoneme were analyzed: Cy3-DNA rod (left) and A647-kinesin (right). Free kinesins, which did not bind the DNA rod, show A647- but not Cy3 signal.

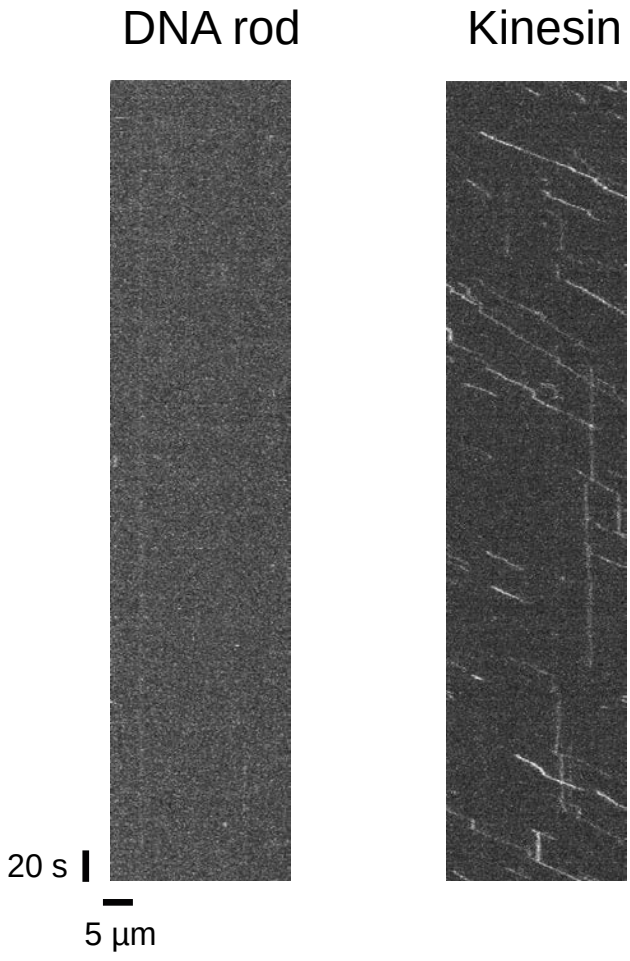

Supplementary Fig. 16. Motility of plain DNA rods was not observed.
Kymograph of the DNA rod in Cy3 channel (left) and kinesin (right). No colocalized spots were observed, showing that the movements observed in other figures were kinesin-dependent motility.

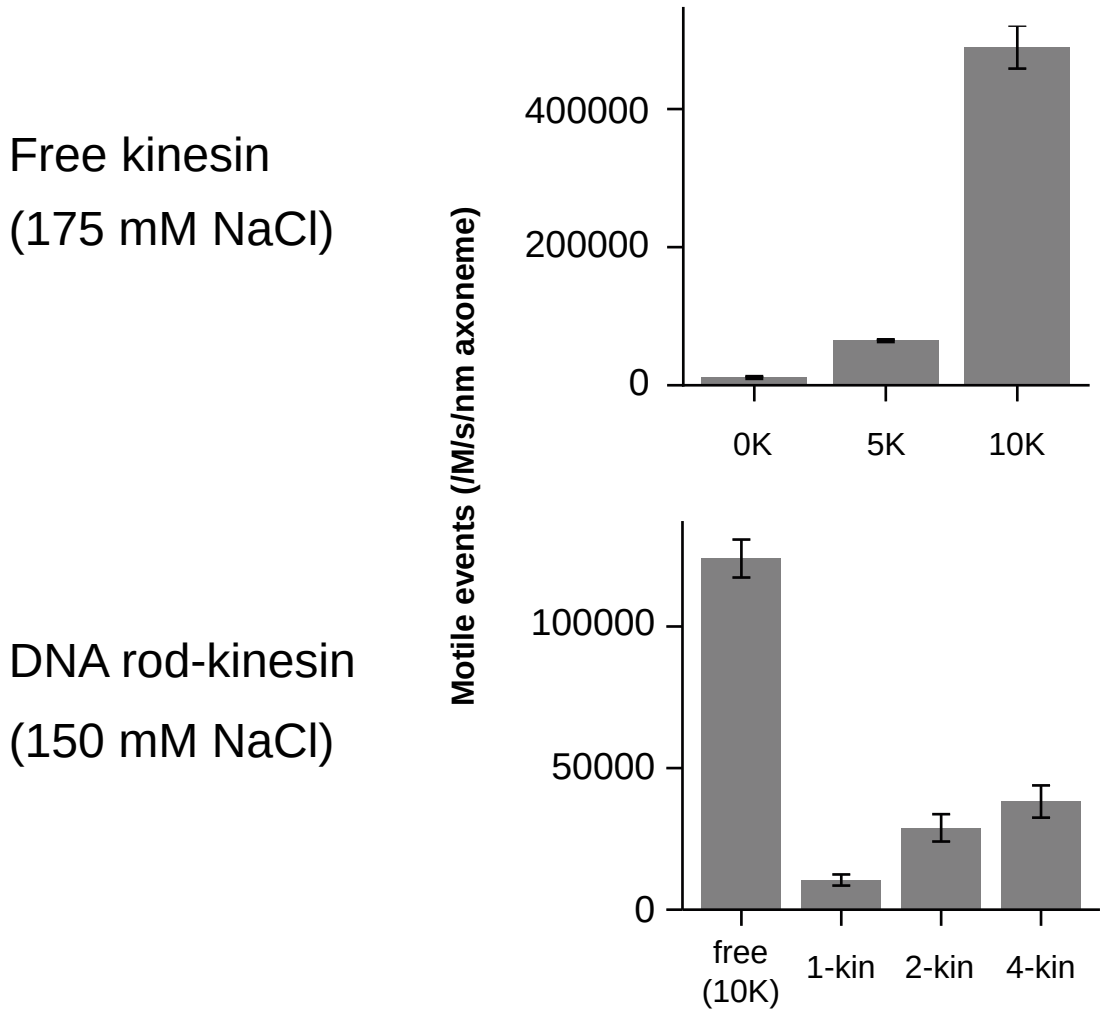

Supplementary Fig. 17. Apparent motile event depends on the number of kinesin molecules. (Upper) For free kinesin, apparent motile events increased with the number of Lys in Lys-tag. (Lower) For the DNA rod-kinesin complex, apparent motile events increased with the number of integrated kinesin molecules. Error bars indicate standard error of averaged data of each axoneme. We noted that estimation of transporter concentration contained 0.5-2-fold error, and therefore, error bar length was corrected.

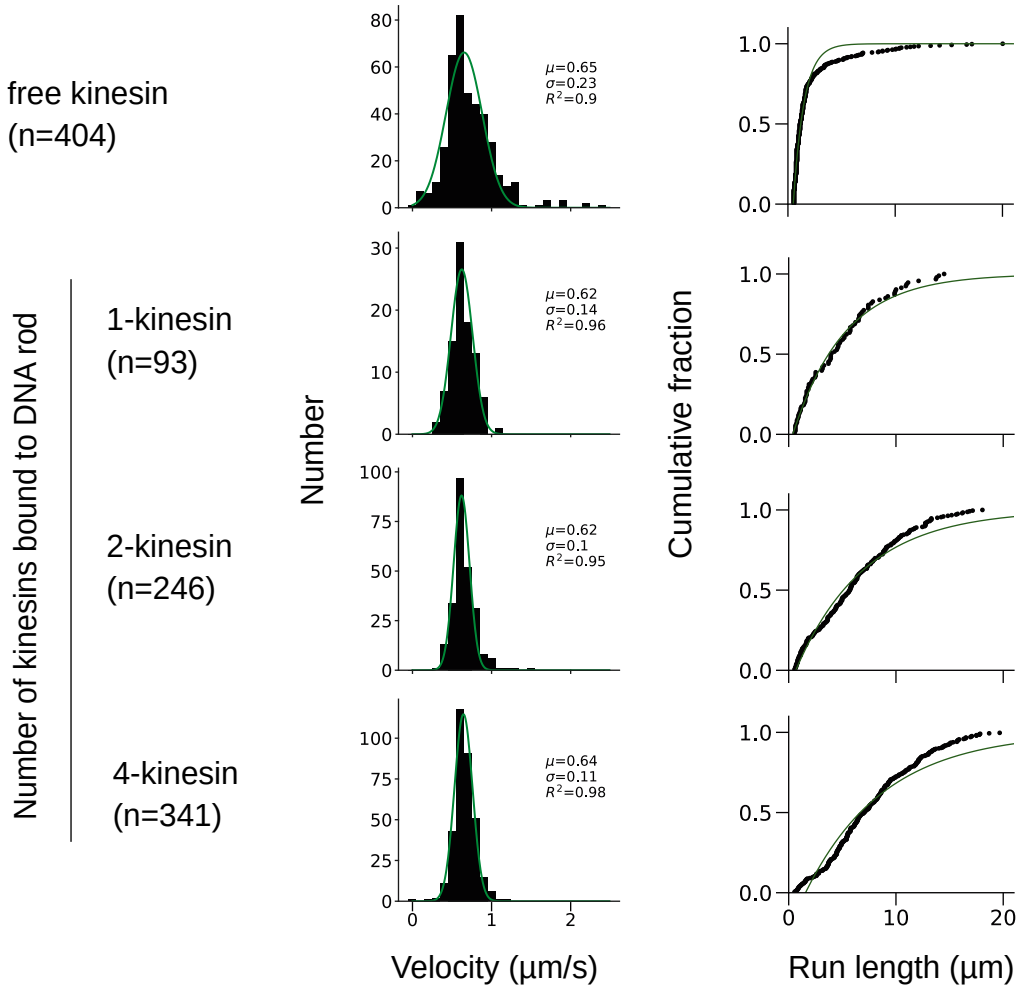

Supplementary Fig. 18. Velocities and run lengths of free kinesin molecules and DNA rods with 1, 2, or 4 kinesin(s) in Fig. 3.
(Left) Histogram of velocities. (Right) Cumulative fraction of run lengths. Line indicates the fitting curve using cumulative distribution function. For analysis, traces of Cy3-DNA rod were used except for data on free A647-kinesin.

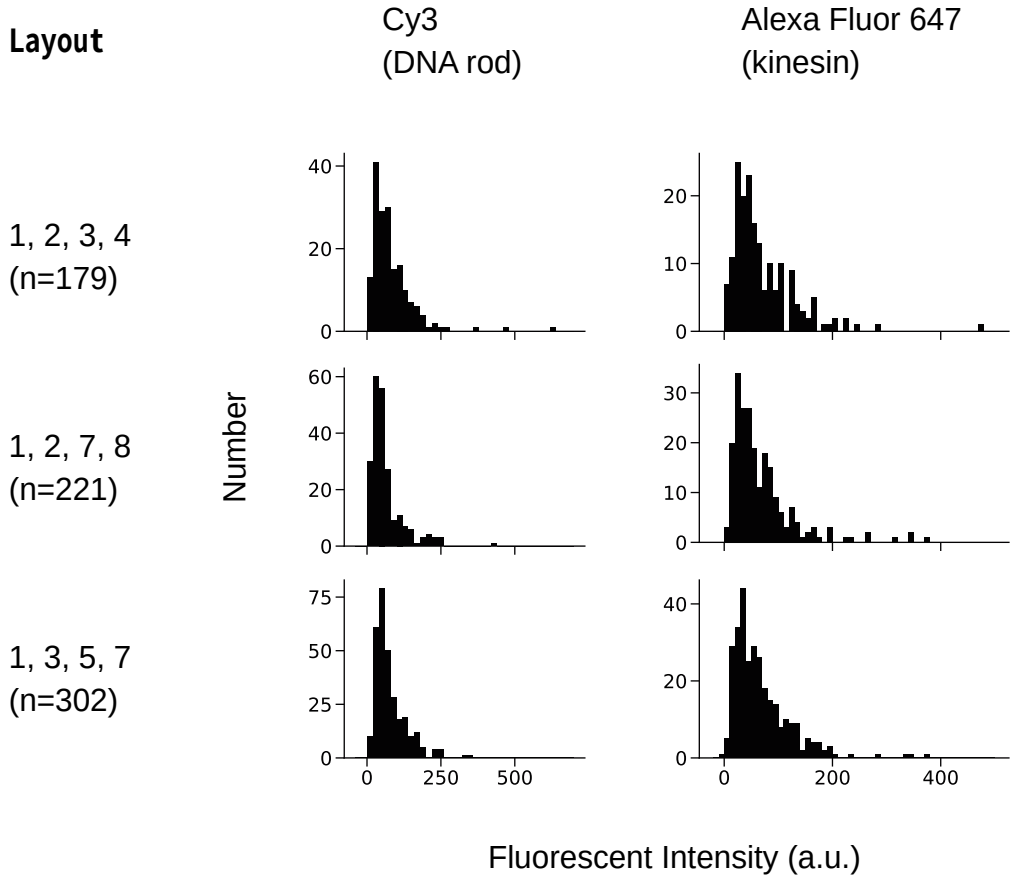

Supplementary Fig. 19. Fluorescence intensity distributions of four-kinesin-occupied complexes in Fig. 4.
Transport complexes with three different layouts moving along an axoneme were analyzed. Both Cy3 (DNA rod, left) and A647 (kinesin, right) intensities were similar, indicating that all three transporter layouts had similar kinesin occupancy. For A647 (kinesin), Kruskal-Wallis test showed no statistically significant difference between layouts (P ~ 0.7).

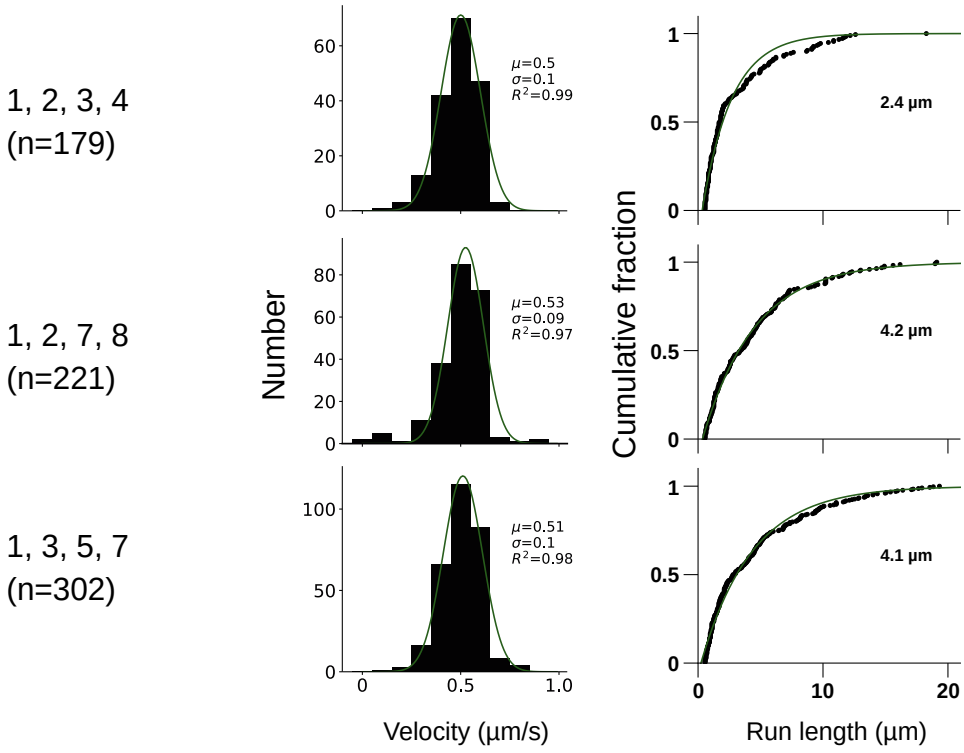

Supplementary Fig. 20. Velocities and run lengths of four-kinesin-occupied complexes in Fig. 4. (Left) Histogram of velocities. (Right) Cumulative fraction of run lengths. Line indicates the fitting curve using the cumulative distribution function. For analysis, traces of Cy3-DNA rod were used.

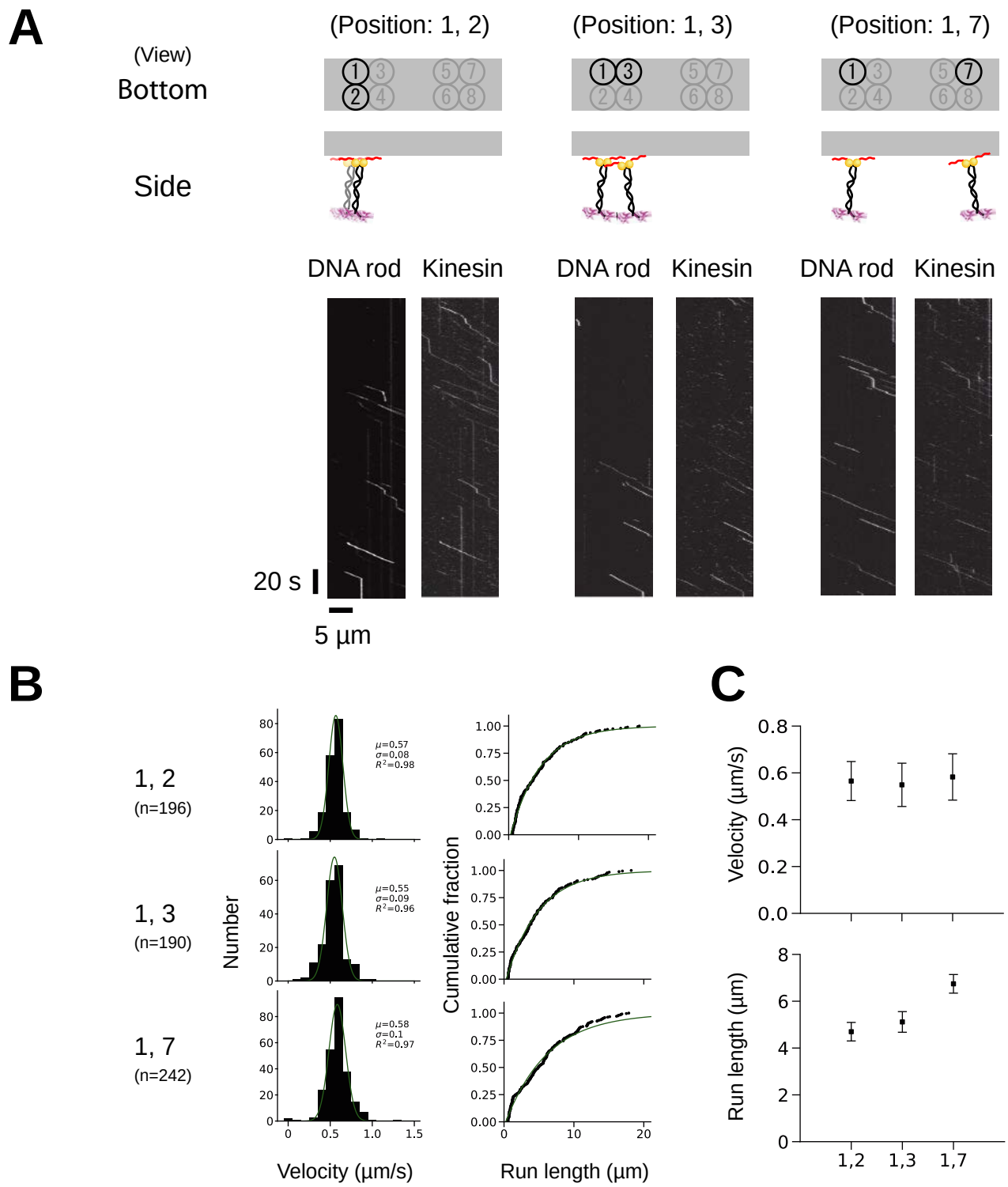

Supplementary Fig. 21. Movements of two-kinesin-occupied complexes.
(A) Kymographs of Cy3-DNA rods with three different layouts of two A647-kinesins. Scale bar for vertical axis = 20 s, horizontal axis = 5 µm. (B) Histograms of velocities (left) and cumulative fractions of run lengths (right). (C) Average velocities (top, $P < 0.001$ [one-way ANOVA]. "1,2-1,3," $P >= 0.05$; "1,2-1,7," $P < 0.05$; "1,3-1,7," $P < 0.001$ [Tukey's test]) and run lengths (bottom, $P < 0.05$ [Kruskal-Wallis test]. "1,2-1,3," $P >= 0.05$; "1,2-1,7," $P < 0.01$; "1,3-1,7," $P < 0.05$ [Conover-Imam test]) of rod-kinesin were statistically different with different kinesin layouts. However, although the *P*-values of velocity were small, the fold change of mean values (µ) was small (< 1.07; fold change = $\mu_{\text{layout A}}/\mu_{\text{layout B}}$, where $\mu_{\text{layout A}}$ refers to µ of the layout with the larger µ value and $\mu_{\text{layout B}}$ is µ of another layout) compared with the error level (SD, SD/µ = 0.09/0.58 = 0.15). The measurements were performed for 210 mM NaCl condition (see methods for detail). Error bars indicate S.D. of total measurements (velocity) or S.E.M. determined by bootstrapping (run length) from two independent experiments (total 6 chambers).

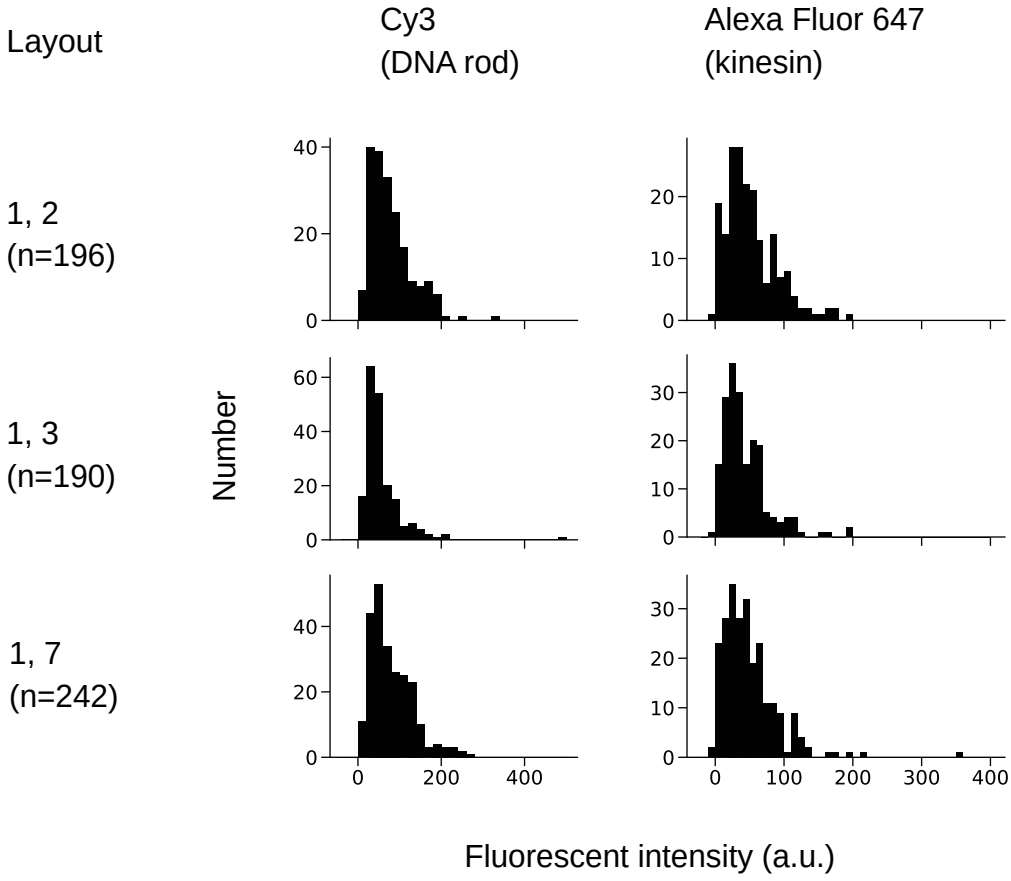

Supplementary Fig. 22. Fluorescence intensity distributions of two-kinesin occupied complexes in Fig. s21.
Transport complexes with three different layouts moving along an axoneme were analyzed. Intensities of both Cy3 (DNA rod, left) and A647 (kinesin, right) were similar, indicating that all 3 layout transporters had similar kinesin occupancy.

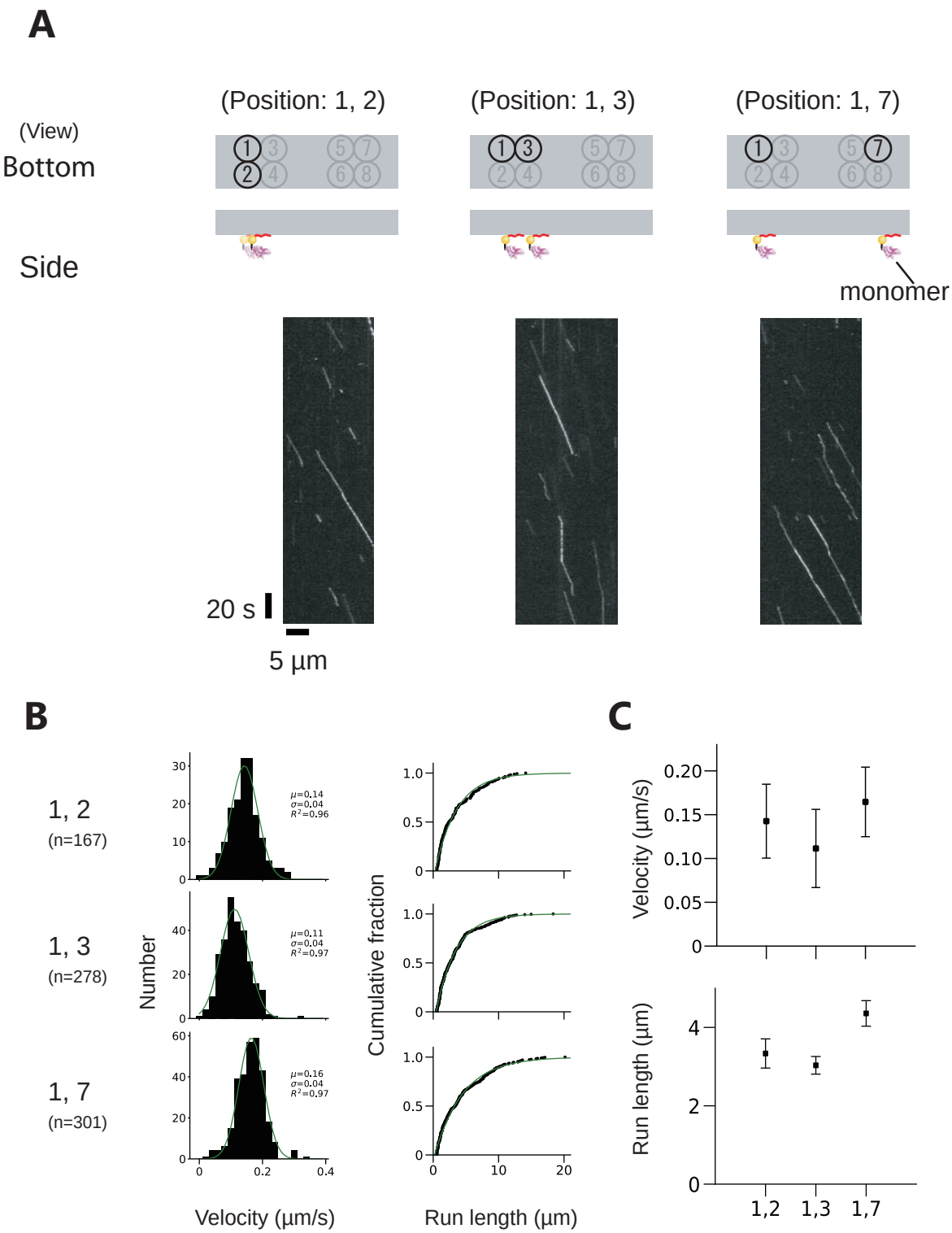

Supplementary Fig. 23. Movements of two monomer kinesin-occupied complexes.
(A) Kymographs of Cy3-DNA rods with three different layouts of two A647-kinesins. Scale bar for vertical axis = 20 s, horizontal axis = 5 µm. (B) Histograms of velocities (left) and cumulative fractions of run lengths (right). (C) Average velocities (top, $P < 0.001$ [one-way ANOVA]. "1,2-1,3," $P < 0.001$; "1,2-1,7," $P < 0.001$; "1,3-1,7," $P < 0.001$ [Tukey's test]) and run lengths (bottom, $P < 0.05$ [Kruskal-Wallis test]. "1,2-1,3," $P >= 0.05$; "1,2-1,7," $P < 0.05$; "1,3-1,7," $P < 0.05$ [Conover-Imam test]) differed with different kinesin layouts. The measurements were performed in 120 mM NaCl condition (see methods for detail). Error bars indicate S.D. of total measurements (velocity) or S.E.M. determined by bootstrapping (run length) from two independent experiments (total 8 chambers).

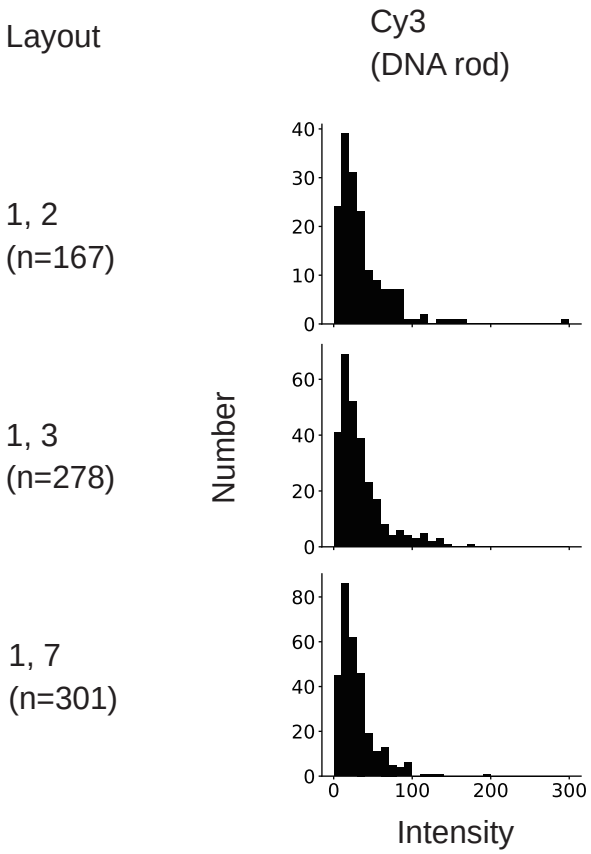

Supplementary Fig. 24. Fluorescence intensity distributions of two-kinesin occupied complexes in Fig. s23.
Transport complexes with three different layouts moving along an axoneme were analyzed. Similar Cy3 (DNA rod) intensities were observed for all 3 layouts.

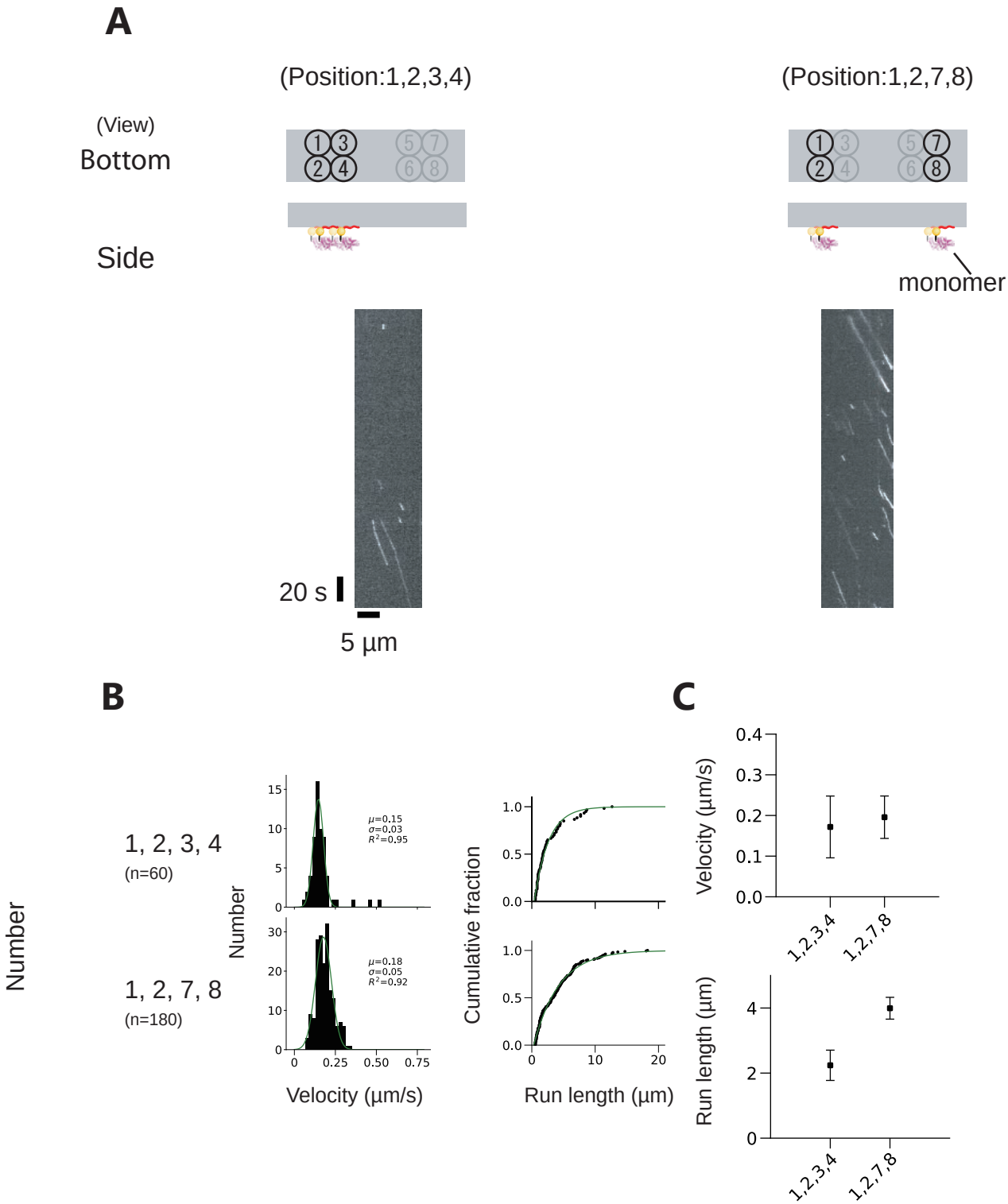

Supplementary Fig. 25. Movements of four monomer kinesin-occupied complexes.
(A) Kymographs of Cy3-DNA rods with two different layouts of 4-monomer-kinesins. Scale bar for vertical axis = 20 s, horizontal axis = 5 µm. (B) Histograms of velocities (left) and cumulative fractions of run lengths (right). (C) Average velocities (top, $P < 0.01$ [Tukey's test]) and run lengths (bottom, $P < 0.05$ [Conover-Imam test]) differed with different kinesin layouts. The measurements were performed in 150 mM NaCl condition (see methods for detail). Error bars indicate S.D. of total measurements (velocity) or S.E.M. determined by bootstrapping (run length) from two independent experiments (total 8 chambers).

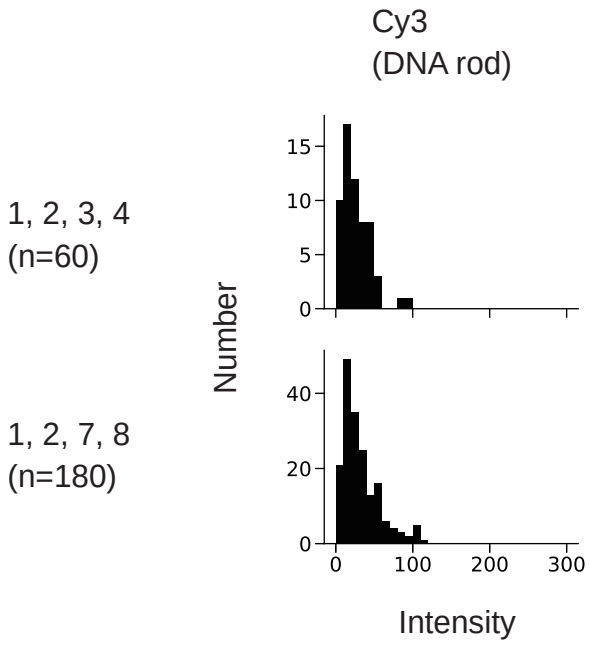

Supplementary Fig. 26. Fluorescence intensity distributions of four-kinesin occupied complexes in Fig. s25.
Transport complexes with two different layouts moving along an axoneme were analyzed. Similar Cy3 (DNA rod) intensities were observed for both layouts.

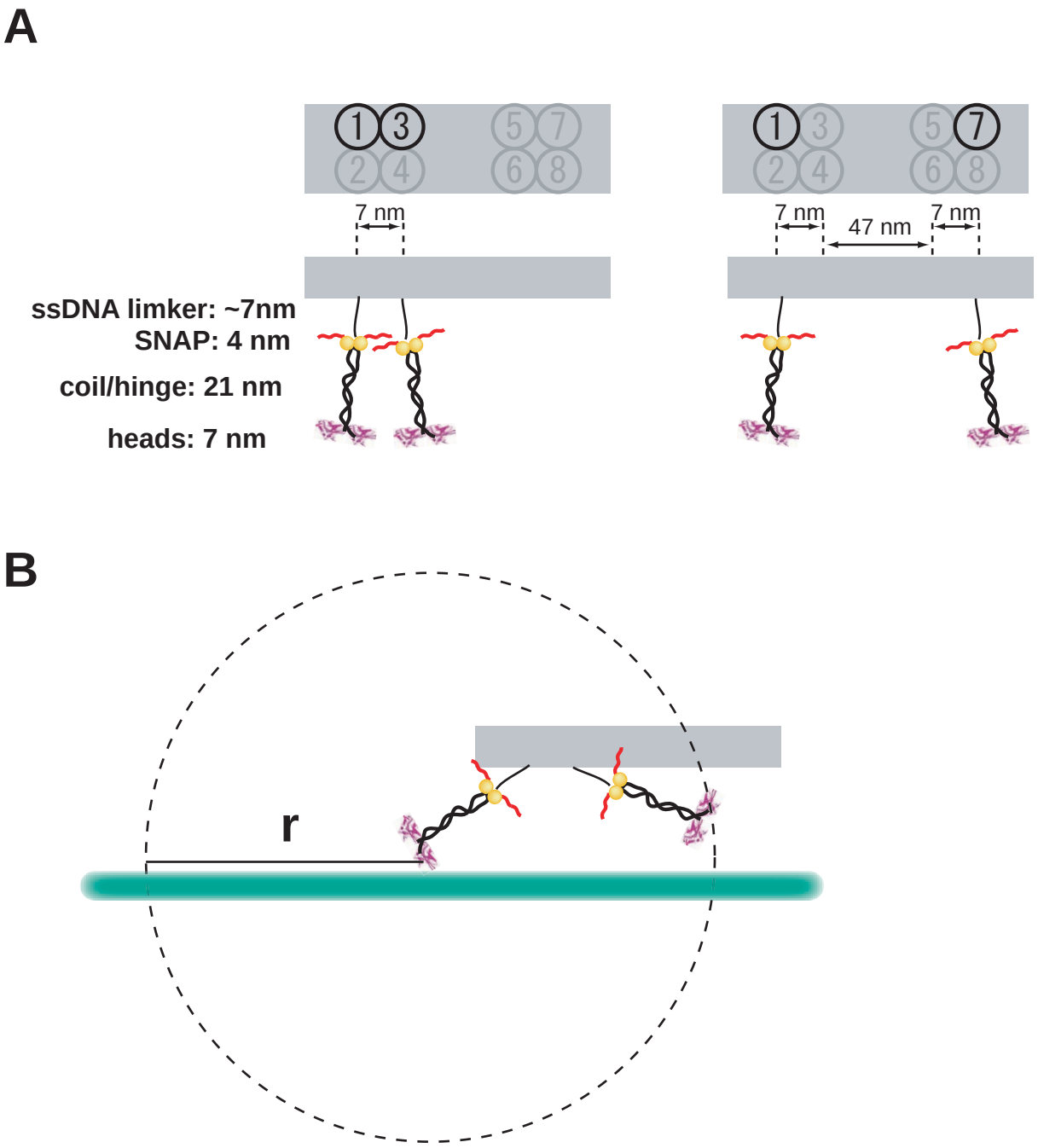

Supplementary Fig. 27. Estimation of effective tubulin concentration.
(A) To-scale diagram of the motor-scaffold complex. Component names and estimated sizes are shown. Estimation is based on the literature (Feng et al., ref#15 and Masubuchi et al., ref#28). Briefly, Neck coil, hinge and coil part is adopted from Feng. et al. (our KIF-5A truncated construct has total 157 a.a. of these regions, which is slightly [45 a.a.] shorter than that of Drosophila KHC truncated used in Feng. et al., [202 a.a.]). Length of ssDNA part is adopted from Masubuchi et al. (0.23 nm/nt under tension applied by T7 RNA polymerase. 30 x 0.23 ~ 7 nm). (B) We calculated the effective local tubulin concentration for a tethered motor based on the literature (Feng et al., ref#15). Briefly, effective concentration was calculated by estimating the number of tubulin subunits accessible in the search volume of the tethered motor. The end-to-end distance between the two motors is approximately 85 nm for position (1,3) as shown in (A). If the tethered motor searches a hemispheric volume above the microtubule, that volume is 1.25 x 10^{-18} L. For a 170 nm length of microtubule in which the top six protofilaments are exposed, there are 128 tubulin subunits (8 nm per tubulin), corresponding to 170 μM tubulin. Similarly the effective tubulin concentration was calculated as 65 μM for position (1, 7), where the end-to-end distance between the two motors is approximately 139 nm.